Desalination and Water Treatment
www.deswater.com
doi: 10.5004/dwt.2022.27943

247 (2022) 216–228
January

Adsorptive removal of tetracycline from aqueous solution by surfactant-modified zeolite: equilibrium, kinetics and thermodynamics

Ferdos Kord Mostafapour[a], Murat Yilmaz[b], Amir Hossein Mahvi[c], Azad Younesi[d], Fatemeh Ganji[e], Davoud Balarak[a,*]

[a]*Department of Environmental Health, Health Promotion Research Center, Zahedan University of Medical Sciences, Zahedan, Iran, email: dbalarak2@gmail.com*
[b]*Osmaniye Korkut Ata University, Faculty of Engineering, Department of Chemical Engineering, 80000, Osmaniye, Turkey*
[c]*Center for Solid Waste Research, Institute for Environmental Research, Tehran University of Medical Sciences, Tehran, Iran*
[d]*School of Environmental Engineering, University of Tehran Aras International Campus, Tehran, Iran*
[e]*Student Research Committee, Zahedan University of Medical Sciences, Zahedan, Iran*

Received 5 August 2021; Accepted 29 October 2021

ABSTRACT

This study was performed for estimating the potential of adsorption technique using surfactant (cetyltrimethylammonium bromide)-modified zeolite (CTAB-Z) for eliminating Tetracycline (TC) from an aqueous solution. The effects associated with variation of included parameters (i.e., the initial TC concentration, temperature, contact time, adsorbent dose, and stirring rate) on TC adsorption efficiency were evaluated. Based on our studies, CTAB-Z could remove 99.8% of TC; this is indicative of the acceptable efficiency of CTAB-Z for adsorption of TC from synthetic wastewater. The equilibrium time for TC adsorption was 90 min. The employment of adsorption isotherms models (e.g., Langmuir, Freundlich, Redlich–Peterson (R-P), Cobble Corrigan (K-C), Dubinin-Radushkevich (D-R) and Temkin) highlighted better fitness of the adsorption data with the Langmuir isotherm, and based on this model, the values of 74.1, 85.1, 97.9, and 108.4 mg/g was obtained for monolayer adsorption capacity of TC at 288, 298, 308, and 318 K, respectively. The results achieved from five desorption regeneration cycles indicated a reduction in the removal efficiencies of CTAB-Z from 99.8% to 89.2%. According to the results of thermodynamic parameters, the spontaneous and feasible nature of the studied process based on $\Delta G° < 0$ was confirmed; however, it was endothermic in nature since a positive value for enthalpy ($\Delta H°$ = 43.84 kJ/mol) was detected. Moreover, based on the values of $\Delta S°$ = 0.652 kJ/mol, the randomness at the solid-liquid interface was improved.

Keywords: Tetracycline; CTAB-Z; Adsorption; Thermodynamics

1. Introduction

In the last decades, the world has been threatened with a new environmental issue, that is, the emerging contaminants in water bodies, which should be severely considered by governments around the world [1,2]. The presence of one of the important types of emerging contaminants, that is, pharmaceuticals in surface water and effluents released from wastewater treatment plants (SWTP) has been documented in various studies [3,4]. The levels of pharmaceutical substances and personal care products in ground and surface water have been detected to be associated with an increasing trend [5,6] and the discharge of effluents has been addressed as the main way to reach waterways [7].

* Corresponding author.

Furthermore, other sources for reaching them into the environment such as direct emissions from the production sites, inappropriate disposal of surplus drugs in households, medical care, and therapeutic treatment of livestock have been reported [8,9]. Since the complete removal of these compounds by sewage treatment plants is not possible and they are ineffective in this case and their presence in receiving water systems is inevitable. Considering the above, a remarkable necessity is detected for applying a suitable treatment method for the effluents containing the pharmaceuticals prior to entry into the receiving waters [10,11].

Many families of antibiotics are used for bacteria treatment [10]. Tetracycline (TC) is a big antibiotic group that is widely used to treat animal and human diseases as well as an antibacterial in aquaculture activity [11,12]. In the TC group, tetracycline (TC), whose molecular structure is shown in Fig. 1, is the most common antibiotic. The TC is widely used to not only treat diseases of animals but also used as a part of animal feed to enhance effective growth [13]. High amounts of TC are released into the aqueous solution that can cause serious problems for animals and human health [14,15]. TC cannot be fully absorbed and metabolized by humans and animals and have low biodegradability, and can potentially cause a variety of adverse effects including acute and chronic toxicity, disruption of aquatic photosynthetic organisms, impact on indigenous microbial populations, and damage to antibiotic-resistant genes in microorganisms [11]. Thus, the presence of TC residues in water poses serious risks to humans and ecology and is a major concern [15].

The typical treatments of wastewaters containing antibiotics are considered to be accomplished partially and inefficiently. Thus, there is a requirement to develop a new beneficial treatments technology [15,16]. To date, there are a lot of techniques, such as filtration, ion exchange, adsorption, electrochemical treatment, membrane separation, catalytic degradation, etc., which have been developed for the removal of antibiotics from wastewater [17,18].

Adsorption is an important technique since it is environmentally friendly, cost-effective, functional, and easy to test, and adsorbent regeneration is also straightforward [19,20]. Synthetic adsorbents are mostly utilized to improve wastewater quality since they are extremely effective at removing pollutants from the aquatic environment [21]. Many synthetic adsorbents, on the other hand, are naturally poisonous and pollute the environment [19]. As a result, there has recently been a lot of interest in pollutants removal studies using natural adsorbents such as algae, clay, rice husk, zeolite, jujube stone, orange peel, etc. [21,22].

In recent years, various studies have been performed using mineral adsorbents such as zeolite, bentonite, montmorillonite, etc. [23]. These compounds have a negative charge on their surface and are not suitable for the adsorption of anionic compounds [24]. Therefore, to increase the efficiency of these adsorbents for removing anionic compounds, the correction method using a surfactant, which gives a positive charge to the adsorbent surface, will be used, which is one of the innovations of this study.

Natural zeolites are crystalline microporous aluminosilicates and have very divergent and exact structures; they contain a framework composed of tetrahedra of SiO_4 and AlO_4 [23,24]. The negative charge on the zeolite framework is formed through isomorphous substitution of Al^{3+} for Si^{4+} in the tetrahedral; the formed negative charge can be balanced by interchangeable cations. So, these substances are cations exchangers [25]. According to reports, the affinity of cationic surfactants for this negative charge is high [26]. Considering this characteristic, studies for upgrading the anion exchange capacity of zeolites have been conducted by adsorbing a cationic surfactant on their external surface. For this purpose, long alkyl chains with a quaternary ammonium group at one end of the chain, such as HDTMA or CTAB, are considered as the most commonly used cationic surfactants [27,28].

In most studies, equilibrium data using regression coefficients are used to match isotherms and kinetics. But employment of regression coefficient alone will not be enough for adaptability. Therefore, for more accuracy, different error coefficients were used in this study.

Thus, the objective of this study is to investigate the availability of CTAB-Z as an adsorbent for the removal of TC from aqueous solutions. For this study, the influence of several factors (e.g., pH, contact time, CTAB-Z mass, temperature, TC concentration, and shaking speed) on the removal efficiency of TC was investigated. The kinetic, isotherm, and thermodynamic models were applied to explain the adsorption behavior. Also, error functions were calculated.

2. Materials and methods

2.1. Materials

The material which was applied as a target pollutant in batch experiments of this research was the tetracycline antibiotic. In fact, the TC hydrochloride (Molecular weight: 480.9, Molecular: $C_{22}H_{24}N_2O_8$-HCl) was obtained from Sigma-Aldrich, USA. As it has been illustrated in Fig. 1, you can see the chemical structure of TC. In order to prepare the stock solution of TC, distilled water was utilized. Other chemical structures which have been used in this experiment were supplied from Merck in Germany. Preparing the stock solution of the studied pollutant, that is, TC was done using 1 g/L in distilled water. The desired solutions were made by attenuating the stock solutions which was done by means of the distilled water to get the desired concentration. The value for the pH of the solutions was approximately 7.

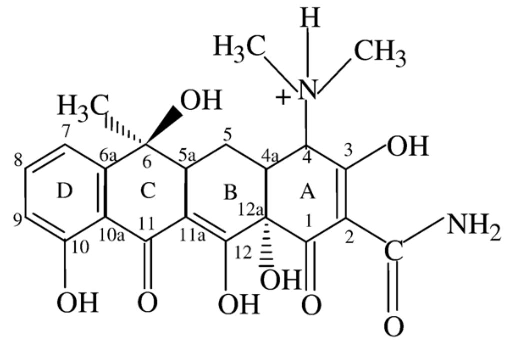

Fig. 1. The chemical structure of tetracycline hydrochloride.

2.2. Preparation and characterization of the CTAB-Z adsorbent

In order to gather the raw zeolite for the experiment, the researchers were referred to one of the local areas in Tabriz, a city in the northwest of Iran. Before measuring, the treatment of zeolite was done as the following statements, to attain the neutral pH, the zeolite was washed and rinsed several times using the ultrapure water. Afterward, it was dried at the temperature of 110°C. Using a desiccator at room temperature, the zeolite was cooled and then it was stored in a container of polyethylene. In order to collect molecules with the size of 60 mesh, which is less than 0.25 mm, the dried zeolite was stirred. The surfactant-modified zeolite was polymerized by the following steps. In this combination, 50 g zeolite was put in 500 mL of water containing 10 g of CTAB. Stirring the reaction components was done at 25°C for 12 h. Then, the resulted chemical product was refined and washed recurrently through the distilled water as long as no bromide could be detected by the $AgNO_3$ solution (0.1 M). Moreover, the CTAB-Z was dried at 110°C for 6 h.

The elemental analysis was carried out by electron microscope (SEM) through operating Oxford instrument (Stereo Scan S360), which is completed by Energy dispersive X-ray (EDX). Surface area and pore size were determined by the analyses of N_2 adsorption-desorption isotherm and BJH using a Micromeritics Analyzer (ASAP 2460) at 77 K. In order to achieve the spectra and to obtain the characteristic peaks in wavenumbers which is varying from 500 to 4,000 cm^{-1}, the researchers employed a Perkin Elmer spectrum 100 FT-IR spectrophotometer. The XRD patterns of CTAB-Z were recorded on a Bruker DS Advance diffractometer at 40 kV and 40 mA utilizing Cu Kα radiation.

2.3. Batch adsorption experiments

In this research, the adsorption experiments were calculated in batch mode. For measuring the TC adsorption kinetics, 100 ml of TC solutions with the initial concentration of 10–00 mg/L were situated in numerous glass tubes, and they were then blended with 1.5 g/L of adsorbents; the pH of the solutions were around 6.9–7. After completing the shaking process, it was centrifuged at 3,600 rpm for 10 min. In order to adjust the pH, HCl and NaOH were applied in the solutions (100 mg/L) to adjust their pH in range of 3–11.

To determine the TC concentration of all samples, HPLC (C18 ODS column) was used by means of a UV detector 2006 at a wavelength of 190 nm. The mobile phase was a mixture of acetonitrile and 0.01 M oxalic acid (30:70 (v/v)), which was utilized at room temperature at a constant flow rate of 1.0 ml min^{-1}. Also, the volume of the injected amount of the mixture was 10mL. The retention time of TC hydrochloride was estimated as 4 min. Besides, in this study, all adsorption experiments were carried out three times, and an average value was designated to the outcomes of the experiments.

Using the equations 1–3 [29,30], the researchers precisely estimated the TC removal percentage and the amount of TC adsorbed per gram of CTAB-Z at time t and equilibrium:

$$\% R = \frac{C_0 - C_e}{C_0} \times 100 \tag{1}$$

$$q_t = \left(C_0 - C_t\right) \times \frac{V}{m} \tag{2}$$

$$q_e = \left(C_0 - C_e\right) \times \frac{V}{m} \tag{3}$$

where V is defined as the solution volume (L); C_0 (mg/L) is known to be the initial concentration of TC, and C_t and C_e (mg/L) are recognized as the concentration at time t and equilibrium concentration in solution, and m is the representative of the CTAB-Z weight (g).

2.4. Regeneration and reusability

The following explanations describe the conditions for doing this experiment; first, 0.3 g CTAB-Z and 100 mg/L TC should be added into the 200 ml conical flask. Then, a sealing film was used to close the bottle mouth. The experiments were performed at a temperature of 25°C and a speed of 200 rpm. Subsequently, when the adsorption was completed, the adsorbent was isolated and washed it many times using the distilled water and then dried it. After drying the adsorbent, it is added to a glass container containing 100 ml of distilled water as the regenerating liquid. It is then subjected to ultrasonic wave for 90 min. Finally, the CTAB-Z is collected, then rinsed with distilled water and continued for further tests, which should be up to 5 times.

2.5. Error analysis

The best isotherm and kinetic model is determined by the correlation coefficient (R^2) analysis. Although this is useful in determining the efficiency of the correlation analysis, this analysis has limitations in solving isotherm and kinetic models that are not inherently linear. Therefore, we used three error functions to find a suitable model to represent the experimental data [31,32]. The error functions used are expressed as Eqs. (4)–(6).

$$\text{Sum of Squared Errors (SSE)} = \sum_{i=1}^{n} \left(q_e \text{ cal} - q_e \text{ meas}\right)_i^2 \tag{4}$$

$$\text{Sum of absolute errors } \left(\text{SAE}\right) = \sum_{i=1}^{n} \left(q_{e,\text{cal}} - q_{e,\text{meas}}\right)_i \tag{5}$$

$$\text{Average relative error}\left(\text{ARE}\right) = \frac{100}{n} \sum_{i=1}^{n} \left(\frac{q_{e,\text{cal}} - q_{e,\text{meas}}}{q_{e,\text{meas}}}\right)_i \tag{6}$$

3. Results and discussion

3.1. Characteristics of CTAB-Z

The results of X-ray diffraction (XRD) and SEM-DEX (energy dispersive X-ray spectrometer) techniques were displayed in Figs. 2a–d. The surface and morphology of the particles were manifested through SEM analysis. Fig. 2a illustrates images of a natural zeolite which have developed partially into crystalline laminar habits. It also shows that conglomerates of compact crystals are different from those of the zeolite crystals which are correspondent to

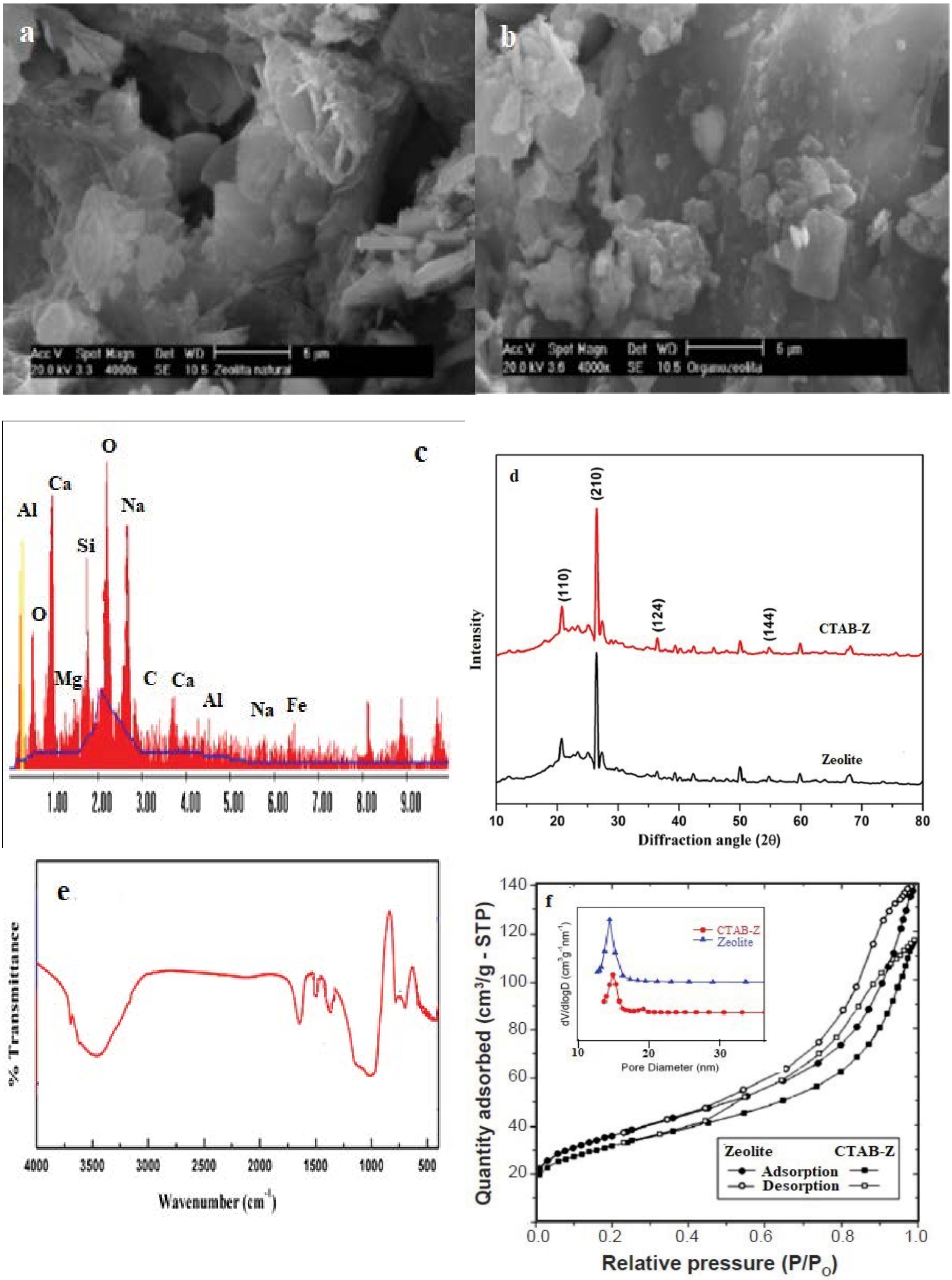

Fig. 2. SEM images of zeolite and CTAB-Z (a-b), XRD pattern of CTAB-Z (b), XRD patterns of Fe_2O_3/B/TiO_2 (c), EDX image of CTAB-Z (d), FTIR image of CTAB-Z (d) N_2 adsorption-desorption isotherms Inset: pore size distributions from the adsorption branches through the BJH method N_2 adsorption-desorption isotherm (f).

determined impurities including feldspar and quartz [25]. In Fig. 2b, the image of the CTAB-Z is displayed, whereas the laminar crystals are not clearly visible due to covering the external surface of the zeolite crystals by surfactant.

This indicated that CTAB-Z is composed of SiO_2 (56.76%), Al_2O_3 (21.82%), K_2O (4.21%), Na_2O (3.83%), Fe_2O_3 (8.89%), CaO (2.55%), MgO (1.44%) and others (1.36%). The peaks at 2θ = 26.64 refer to one of the components of CTAB-Z known as SiO_2 (quartz). Other studies also obtained and reported the same results, which were detected in this study on CTAB-Z [25].

The XRD patterns for pure zeolite and CTAB-Z nanoparticles are given in Fig. 2d. The characteristic peaks at diffraction angle, 2θ = 20.8°, 26.6°, 36.4°, 54.8° corresponds to the planes (110), (210), (124), and (144) of the bentonite material. These XRD patterns are in good agreement with the standard JCPDS file (card no.01-088-0891). From the graph, it can be observed that there is neither a significant change in intensity of the patterns, nor there is a shift in the peaks. This behavior is due to no significant change in the phase structure of material after the modification.

In Fig. 2e, the IR spectrum of CTAB-Z can be seen clearly. The strong bands at 3,300 to 3,725 cm^{-1} can be attributed to the asymmetric stretching vibration of the NH_2 group. The band, which runs between 1,600 and 1,700 cm^{-1}, is attributed to the vibrations of valence of the OH group of water constitution. The asymmetric and symmetric stretching CN2 vibrations are designated to bands at 1s,470 and 1,413 cm^{-1} sequentially. The allocation of C=S stretching frequency in compounds which contain nitrogen alters in a broad range of 550–1,\100 cm^{-1}.

Nitrogen adsorption-desorption analysis: according to the classification of the International Union of Pure and Applied Chemistry (IUPAC), CTAB-Z and zeolite showed isotherms with a profile similar to type IV isotherms (Fig. 2f). A hysteresis loop and a limit of adsorption in the region of high relative pressure (plateau) are features of these isotherms. The hysteresis loop of isotherms was H3-type, which indicated the presence of slit-shaped pores.

In short, the profile of isotherms and their hysteresis loops indicated that the adsorbents had a porous structure formed mainly by mesopores, associated with some micropores, predominantly with slit-like format. For CTAB-Z, the pore volume and BET surface area are equal to 0.141 cm^3/g and 96.9 m^2/g, respectively. The BET surface area of zeolite composite is 104.2 m^2/g and total pore volume 0.156 cm^3/g. The decrease in adsorption level for CTAB-Z is due to the entry of surfactant into the pores of zeolite.

3.2. Effect of factors

The amount of TC removed by adsorption is strongly dependent on the initial TC concentration. Figs. 3a and b illustrate the variations in the removal percent and amount of TC adsorbed using different values of CTAB-Z. The amount of TC removed was often very high during the first stage of the adsorption process, then gradually decreased until achieving equilibrium. It was also discovered that after reaching equilibrium, contact time had no discernible effect on the adsorption process. The rapid removal rate at this stage is due to the presence of a large number of uncovered active adsorption sites on the CTAB-Z surface in the early adsorption process [33]. The uncovered sites become fully occupied by the adsorbed TC molecules as the time of contact between adsorbent and adsorbate increases, and the repulsive force that occurs between the TC molecules on the surface of adsorbents and TC molecules in the bulk liquid phase reduces the TC adsorption rate [34,35]. The TC removal % reduces as the initial TC concentration is increased. The increased amount of TC absorbed by the adsorbent with raising the initial TC concentration is due to the greater driving force for mass transfer at a raised starting TC concentration [36].

The influence of CTAB-Z mass on TC removal percentage was examined to determine the optimal adsorbent dosage for the greatest efficiency. Fig. 4 shows the percentage of TC removed as a function of adsorbent dosage. The effect of CTAB-Z dose was examined at the

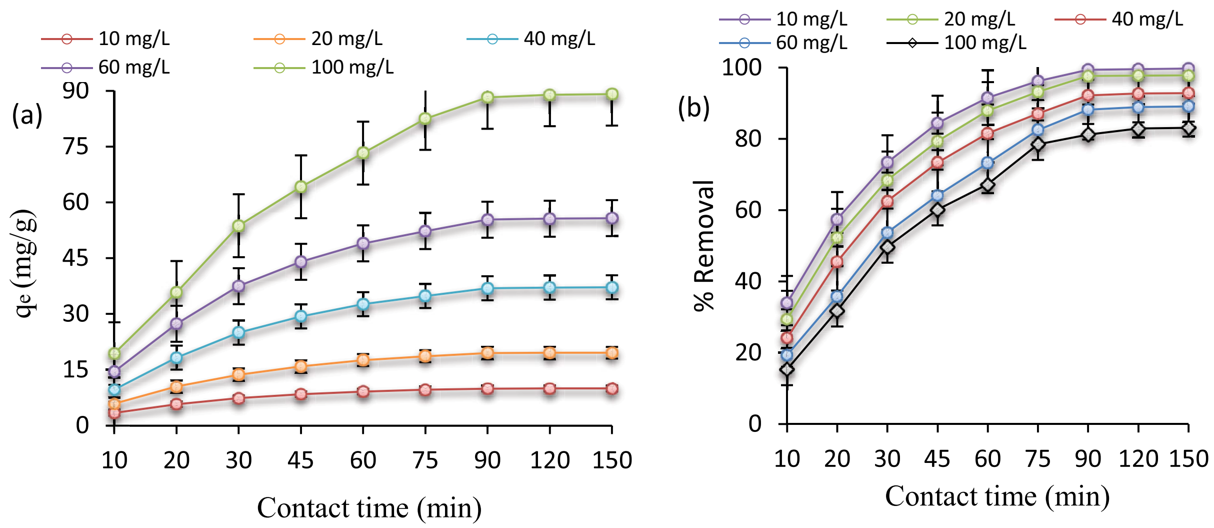

Fig. 3. Effect of contact time and concentration on equilibrium adsorption uptake (a), Effect of contact time and concentration on TC removal (b) (Stirring rate = 200 rpm, pH = 7, Tem: 25°C and adsorbent dose = 1 g/L).

dose between 0.02 to 0.3 g in 100 mL aqueous solution. The results are shown in Fig. 8 that with increasing the CTAB-Z dose from 0.02 to 0.2 g, the removal percentage also increases from 18.5% to 84.2%. Consequently, it was found out that the availability of a larger surface area and more adsorption sites accelerates with an increase in the adsorbent dose [37,38]. Increasing the adsorbent dose over 0.2 g resulted in a minor change in the removal percent. The establishment of a dense screening layer at the adsorbent surface as a result of the accumulation of CTAB-Z particles and a decrease in the distance between the CTAB-Z molecules, known as the screening effect, which happens with a greater adsorbent dose, could explain this phenomenon [39]. The binding sites were hidden from TC molecules by the condensed layer on the adsorbent surface. Furthermore, because CTAB-Z overlapped, TC molecules competed for a limited number of accessible binding sites. Agglomeration or aggregation at higher CTAB-Z dosages lengthens the diffusion channel for TC adsorption, lowering the adsorption rate [40].

In order to analyze the stirring rate effect in adsorption kinetic behavior, % removal values were plotted and the results are shown in Fig. 5. As the stirring rate increases, the removal percentage also increases, and this increase continues up to the 200 rpm stirring rate. The outcome can be considered as the effect of a rise in turbulence and the reduction in boundary layer thickness around the adsorbent molecules which is due to the rise in the degree of mixing. It can also infer that the rate-limiting step in this process was external mass transfer [41].

The surface charge of adsorbents and adsorbate species are determined according to solution pH value, which has an amazing effect on the act of adsorption. Considering Fig. 6, there would be no striking alteration in the amount of adsorption even if the pH increases from 3 to 7. However, the adsorption capacity will decline from 28.9 to 12.5 mg/g if the pH increases from 7 to 11. Particularly if the pH reaches 11, the removal value will achieve 49.4%. This reaction can be attributed to characteristics of CTAB-Z and the ionization features of TC, which is based on the dissociation constants (pKa) of TC. The TC has been identified to be an amphoteric molecule, which has multiple pKa and, at different pH values, it can found different chemical states [13], so that it is in form of H_4TC^+ for pH < 3.4; in form of H_3TC for 3.4 < pH < 7.7; in form of $H2TC^-$ for 7.7 < pH < 9.7, and in form of HTC^{2-} for pH > 9.7 (Fig. 10 insert). The pH_{pzc} of CTAB-Z was 7.8. Therefore, when the PH decreases to pH < 7.8, the electrostatic attraction between TC and CTAB-Z will increase. Moreover, the negative charge of CTAB-Z and the positive charged and uncharged TC molecule (H_4TC^+ or H_3TC) at pH values between 3 and 7 paves the way for the electrostatic attraction and leads to an enormous TC capacity. On the other hand, the negative charge of CTAB-Z and TC molecular (H_2TC^- or HTC^{2-}) at pH values between 7 and 11 enables the electrostatic repulsion and as the result, the capacity of TC will be lowered down. Subsequently, this result proposes that one of the mechanisms of TC adsorption on CTAB-Z was electrostatic attraction.

3.3. Effect of contact time and adsorption kinetics

The contacting time and its effect were examined under certain conditions. Figs. 3a and b show that at the start of the evaluated process, the rate of the process raised

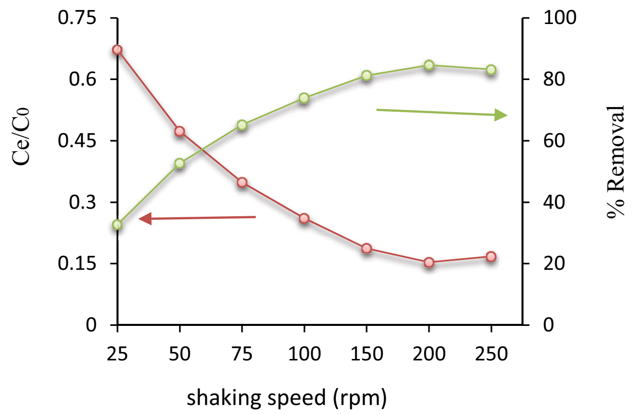

Fig. 5. Effect of stirring rate (C_0 = 100 mg/L, pH = 7, time = 90 min, temperature: 25°C and adsorbent dose = 1.5 g/L).

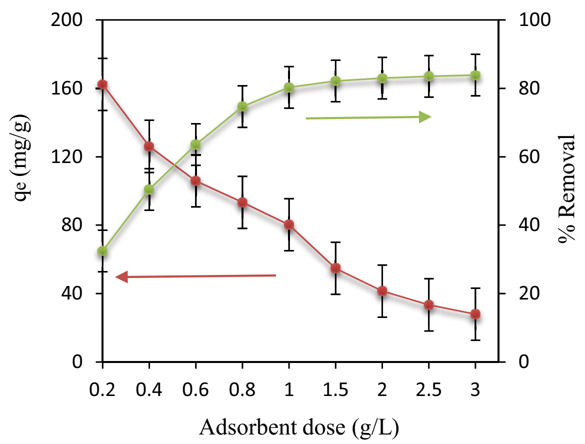

Fig. 4. Effect of adsorbent dose (C_0 = 100 mg/L, pH = 7, time = 90 min and temperature: 25°C and stirring rate = 200 rpm).

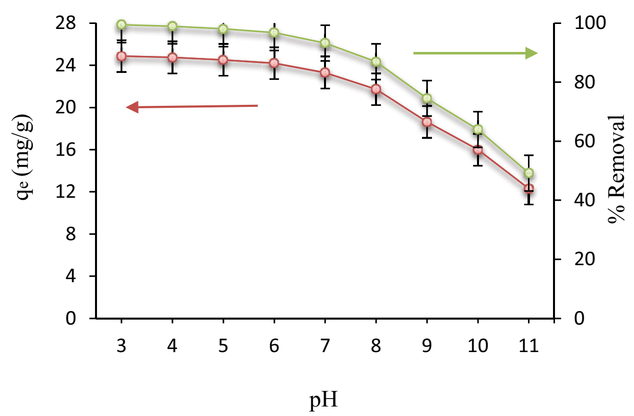

Fig. 6. Effect of pH (C_0 = 25 mg/L, pH = 7, time = 90 min, temperature: 25°C and adsorbent dose = 1.5 g/L).

rapidly. Unlike, when the contact time is extended the process decreases until it reaches equilibrium. According to the results, 90 min was found to be the equilibrium time. This reaction has resulted mainly since the TC concentration in the solution was high initially, and there were abundantly accessible sites on CTAB-Z for adsorption of pollutant [42]. As the adsorption advances, the adsorption rate dwindled slowly because the mentioned sites on the adsorbent surface were slightly full filled by contaminants [43]. Under definite experimental conditions, various adsorption kinetics experiments were accomplished with various contact time. Inspection of adsorption kinetics was done by three models, that is, pseudo-first-order (PFO), pseudo-second-order (PSO), and intra-particle diffusion (IPD) models represented by the following equations [44,45]:

$$\mathrm{Log}\left(q_e - q_t\right) = \log q_e \frac{K_1}{2.303} t \tag{7}$$

$$\frac{t}{q_t} = \frac{1}{k_2 q_e^2} + \frac{t}{q_e} \tag{8}$$

$$q_t = K_d t^{0.5} + C \tag{9}$$

In this equation, K_1 (min^{-1}) and K_2 (g/mg min) are the emblems of the rate constant.

PFO, PSO models were implemented to suitably designate the experimental data (Table 1 and Fig. 7a). The value of the correlation coefficient R^2 for the PSO adsorption model was relatively high (>0.997) at all concentrations. The error coefficient for the PSO kinetics is less than the PFO kinetics. Also, q_e (calculated) using the PSO model is equal to that obtained experimentally. Thus, based on these results, CTAB-Z clearly followed PSO reaction kinetics in the removal of TC from an aqueous solution.

By plotting the kinetics data according to the IPD model (Eq. 9), it is found that the kinetics adsorption of TC onto CTAB-Z consists of three consecutive phases, as shown in Fig. 7b: bulk diffusion, film diffusion, and pore diffusion. In fact, the first phase observed at time between 10 to 30 min ($3 < t^{0.5} < 5.5$) represents the surface and IPD processes, the second phase observed at time between 30 to 75 min ($5.5 < t^{0.5} < 10$) represents liquid film diffusion, and the third phase observed at times higher than 75 min ($10 < t^{0.5} < 13$) represents the diffusion of TC molecules through pores to the active sites of CTAB-Z; then, equilibrium conditions are achieved. In the present study, the first phase is modeled as a term in the IPD model. This is an important step in adsorption studies, as the IPD model provides information about the role of the IPD rate in controlling adsorption.

The linear plot of q_t vs. $t^{1/2}$ does not pass through the origin; therefore, boundary layer diffusion occurs during

Table 1
The results of kinetic model studies related to the TC adsorption onto CTAB-Z

Model	Parameters	10 mg/L	25 mg/L	40 mg/L	60 mg/L	100 mg/L
	$q_{e,\exp}$	9.97	19.5	37.1	53.4	83.1
PFO	$q_{e,\mathrm{cal}}$	2.19	5.94	11.4	27.4	48.5
	K_1	0.059	0.067	0.074	0.085	0.093
	R^2	0.812	0.851	0.843	0.889	0.914
	SSE	7.25	9.32	11.6	10.2	9.25
	SAE	9.84	10.2	9.24	14.3	10.7
	ARE	11.2	9.25	7.27	7.56	8.23
PSO	$q_{e,\mathrm{cal}}$	11.6	23.8	44.6	63.9	85.1
	K_2	0.0042	0.0028	0.0012	0.0008	0.0006
	R^2	0.998	0.998	0.997	0.996	0.995
	SSE	2.26	2.17	1.32	1.06	2.36
	SAE	1.76	1.39	1.18	1.25	2.06
	ARE	1.53	1.06	1.64	1.73	1.35
IPD	Stage 1					
	K_b	4.11	7.29	13.4	15.3	19.4
	C	1.19	4.72	8.25	13.2	25.6
	R^2	0.9514	0.959	0.946	0.932	0.951
	Stage 2					
	K_b	1.06	2.06	4.11	6.24	7.21
	C	6.14	14.6	34.8	41.2	61.4
	R^2	0.931	0.977	0.969	0.923	0.926
	Stage 3					
	K_b	0.17	0.396	0.5729	0.621	0.723
	C	9.27	25.9	51.2	67.2	73.3
	R^2	0.912	0.956	0.972	0.921	0.925

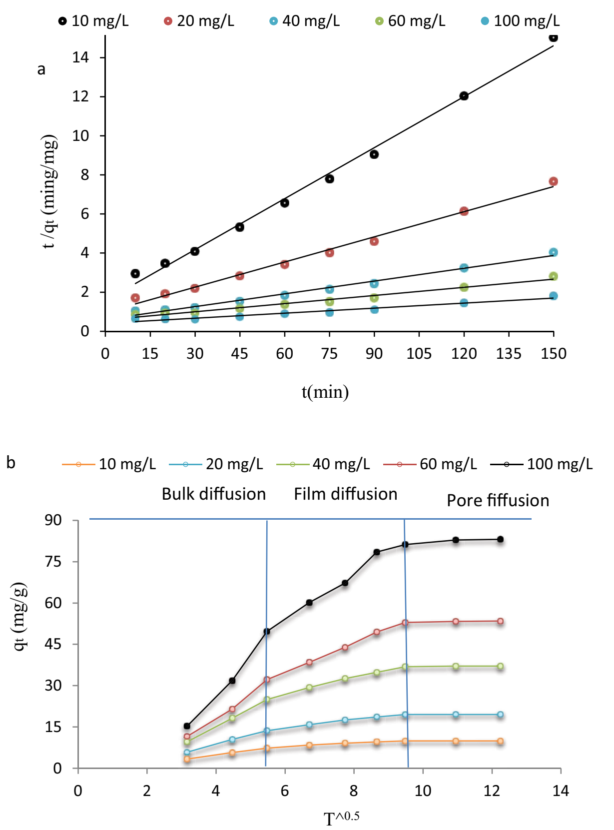

Fig. 7. PSO, (a) IPD kinetic plots for adsorption of TC on CTAB-Z (b).

the adsorption process. The positive values of C for all TC concentrations are indicative of involving the IPD in the adsorption process; nevertheless, the adsorption process is governed not only by IDP as the rate-limiting step but also by other factors controlling TC adsorption on CTAB-Z.

3.4. Effect of temperature and thermodynamic study

As Fig. 8 illustrates, the experiments for studying the changes in the studied process as a function of temperature were implemented at 15, 25, 35, and 45°C (288–318 K). The resulted statistics showed that the altering ratio of the TC on CTAB-Z adsorption is in accordance with the increasing temperature. The rise in temperature causes the rise in the adsorption ratio of TC on CTAB-Z, which exhibited that the process has endothermic nature, and increasing the temperature was effective in development of the TC adsorption [46]. The other hypothesis claimed that when the temperature rises up, there would be an enhancement in nearby sites and structure and volume of the pores on the studied adsorbent surface, therefore the adsorption properties of the adsorbents would be boosted up [47]. The thermodynamics studies were also considered for the conducted adsorption process. The thermodynamic parameters including entropy ($\Delta S°$), enthalpy ($\Delta H°$), standard Gibb's free energy ($\Delta G°$) were obtained using Eqs. (10) and (11) [48].

$$\Delta G° = -RT \text{ Ln } K_L \tag{10}$$

$$\text{Ln } K_L = \left(\frac{\Delta S°}{R}\right) - \left(\frac{\Delta H°}{RT}\right) \tag{11}$$

In this equation, K_L (L/mol) resembles the Langmuir constant. R stands for the gas constant (8.314J/mol K), T is the absolute temperature (K), $\Delta H°$ (kJ/mol) and $\Delta S°$ (kJ/mol K) were considered as the gradient and intercept of the plot of LnK against $1/T$ (Fig. 9). $\Delta S°$, $\Delta G°$, and $\Delta H°$ are significant parameters in evaluating the thermodynamics of the adsorption systems (Table 2). The negative $\Delta G°$ value demonstrates that the adsorption process occurs spontaneously and feasibly [49,50]. Further decrease at $\Delta G°$ from –3.32 to –12.91 kJ/mol, with increasing temperature from 288 to 318 K shows that the driving force will increase the adsorbent uptake level when the temperature is high. Positive $\Delta S°$ (0.652 KJ/mol) suggests that there is an augmented randomness at the adsorbate–adsorbent interface. Also, the positive $\Delta H°$ = 83.84 KJ/mol confirms the process to be endothermic [51].

3.5. Adsorption isotherms

3.5.1. Langmuir isotherm

This isotherm model has been employed profitably for studying the adsorption of various pollutants and has been the most broadly applied sorption isotherm for the sorption of a solute from a liquid solution. The saturated monolayer isotherm can be illustrated as [52]:

$$\frac{1}{q_e} = \frac{1}{q_m K_L} \times \frac{1}{C_e} + \frac{1}{q_m} \tag{12}$$

In this equation, K_L is the representative of a constant related to the affinity of the binding sites and energy of adsorption (L/mg).

3.5.2. Freundlich isotherm

An empirical equation that explains the adsorption onto the heterogeneous surface is known as the Freundlich isotherm. The Freundlich isotherm is generally shown as [53]:

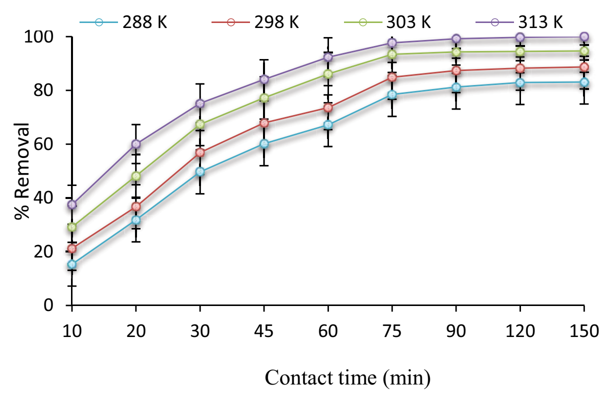

Fig. 8. Effect of temperature (C_0 = 100 mg/L, pH = 7 and adsorbent dose = 1.5 g/L).

Table 2
Values of thermodynamic parameters for the adsorption of TC onto CTAB-Z

Temperature (K)	$\Delta G°$ (kJ/mol)	$\Delta H°$ (kJ/mol)	$\Delta S°$ (kJ/mol K)
288	–3.32	43.84	0.652
298	–4.64		
308	–7.07		
318	–12.91		

$$\text{Ln}\, q_e = \frac{1}{n}\text{Ln}C_e + \text{Ln}K_F \tag{13}$$

where K_F (mg/g (mg/L)$^{1/n}$) is representing the Freundlich constants related to the adsorption capacity and n reveals adsorption intensity of the sorbent.

3.5.3. R–P isotherm

The three-parameter R–P equation, which has a linear dependence on concentration in the numerator and an exponential function in the denominator, has been introduced to advance the fit by the Langmuir or Freundlich equation and is conveyed by the following equation [54]:

$$\text{Ln}\frac{AC_e}{q_e^{-1}} = g\,\text{Ln}\,C_e + \text{Ln}\,B \tag{14}$$

In the above equation A, B and g embody the R-P parameters; the values of g variable between 0 and 1. When g is equal to 1, above equation converts to the Langmuir form.

3.5.4. K-C isotherm

This model, which is also a three-parameter equation, exhibits the equilibrium adsorption data; this model is a combination of the Langmuir and Freundlich isotherm type models and is described by following equation [55]:

$$\frac{1}{q_e} = \frac{1}{\text{AC}_e^n} + \frac{B}{A} \tag{15}$$

In the above equation A, B and n are indicative of the K-C parameters.

3.5.5. Temkin isotherm

The Temkin model is explained according to the following equation [56]:

$$q_e = A + B\,\text{Ln}\,C_e \tag{16}$$

In the mentioned model A and B are signified as isotherm constants.

3.5.6. D-R isotherm

The D–R model is expressed as following equation [57]:

$$\text{Ln}\,q_e = \text{Ln}\,q_m - K\varepsilon^2 \tag{17}$$

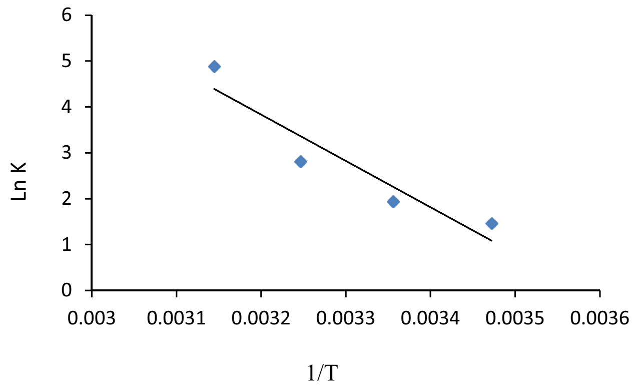

Fig. 9. Van't Hoff plot for determine thermodynamic parameters.

where K indicates the adsorption energy constant, and ε is the Polanyi potential, calculated from Eq. (18) [47]:

$$\varepsilon = RT\,\text{Ln}\left(1 + \frac{1}{C_e}\right) \tag{18}$$

The mean free energy of adsorption, E (kJ/mol), was calculated using Eq. (19) [58]:

$$E = \frac{1}{\sqrt{2K}} \tag{19}$$

Parameters of the six models along with regression coefficient and error coefficient were listed in Table 3. Based on the regression coefficient and error coefficients presented, the best isotherm model was the Langmuir model, because it had a lower error coefficient and a higher regression coefficient. Considering Table 3, when the temperature rises, the K_L, q_m, and K_F were all increased. According to mentioned findings, the adsorption of TC by CTAB-Z from aqueous solutions can effortlessly occur.

The Langmuir constant (K_L) denotes the affinity for the binding of TC. In other words, when the K_L value is high, the affinity will be high too. As stated in Table 3, the monolayer or maximum adsorption capacity (q_m) of CTAB-Z is raised in accordance with the condition in which the temperature goes up. The values of q_m, which were calculated include the numbers of 74.16, 85.19, 97.93, and 108.4 mg/g at 288, 298, 308, and 318 K, respectively. The highest adsorption capacity (q_e) of TC resulting from diverse adsorbents is shown in Table 4.

The investigation of the data manifested that the two isotherms (R-P and K-C) were applicable explanations of the data for adsorption of TC at the evaluated concentration ranges. The g and n constants were approximately 1, which implied that the isotherms were reaching the Langmuir form.

Table 3
Isotherm parameters for TC adsorption onto CTAB-Z

Models	Langmuir				Models	Temkin			
Temp.	288 K	298 K	308 K	318 K	Temp.	288 K	298 K	308 K	318 K
q_m	74.1	85.1	97.9	108.4	A	8.11	10.4	11.6	13.4
R^2	0.994	0.998	0.998	0.997	B	1.72	1.94	2.06	2.14
R_L	0.571	0.623	0.646	0.726	R^2	0.859	0.874	0.884	0.841
SSE	1.45	1.76	3.21	1.45	SSE	6.11	11.7	10.2	12.3
SAE	2.71	1.35	2.46	2.08	SAE	8.25	6.98	9.41	7.24
ARE	1.52	1.49	1.26	1.93	ARE	10.2	9.23	8.14	7.58
Models	R-Peterson					K–Corrigan			
A	9.64	11.6	12.8	12.9	A	6.45	6.772	7.195	7.273
B	0.712	0.949	1.14	1.32	B	0.244	0. 282	0.314	0.396
g	0.532	0.471	0.386	0.314	n	0.334	0.295	0.246	0.196
R^2	0.912	0.924	0.935	0.946	R^2	0.931	0.908	0.902	0.904
SSE	8.24	7.25	7.14	9.24	SSE	4.25	10.6	8.41	6.14
SAE	6.18	8.65	6.24	10.2	SAE	7.11	8.25	8.39	9.25
ARE	7.41	11.9	9.32	11.6	ARE	9.31	7.11	7.37	6.31
Models	Freundlich				Models	D-R			
K_F	2.45	3.12	3.68	4.58	q_m	56.2	72.1	83.4	91.3
$1/n$	0.41	0.52	0.58	0.712	E	3.27	5.18	6.56	7.76
R^2	0.824	0.827	0.852	0.914	R^2	0.926	0.935	0.941	0.931
SSE	9.25	9.24	7.31	10.2	SSE	6.24	7.11	8.32	6.07
SAE	11.27	11.23	8.98	11.6	SAE	11.2	7.24	9.34	5.13
ARE	14.31	6.65	9.23	12.1	ARE	8.21	7.21	8.02	9.06

Table 4
The comparison of adsorption capacity of different adsorbents for TC

Adsorbent	q_e, mg/g	Ref	Adsorbent	q_e, mg/g	Ref
Ferric-activated SBAC	54.33	[42]	Palygorskite	46.21	[39]
Bio-char	36.5	[43]	MWCNT	78.12	[45]
Activated carbon	252.6	[44]	Kaolinite	27.4	[41]
Magnetic Fe_3O_4-graphene	46.54	[38]	Titania	56.81	[40]
Graphene oxide	38.9	[13]	Montmorillonite	71.38	[29]
CTAB-Z at 323 K	108.4	This work	Ferric-activated sludge	43.5	[44]

If the value is in the range of 8–16 KJ/mol, the adsorption type can be explained by ion exchange, and if $E < 8$, the adsorption type is physisorption [59]. The value of E calculated in this study at low temperatures was below 8 KJ/mol. This implies that the type of adsorption involved in this study is physisorption (physical sorption), which usually takes place at low temperatures, but with increasing temperature, chemical adsorption also occurs.

3.6. Desorption regeneration of CTAB-Z

For probing the reusability of CTAB-Z, the pollutants which were adsorbed on CTAB-Z surface were desorbed by ultrasonic vibration. According to Fig. 10, the removal efficiencies of CTAB-Z decreased from 99.8% to 89.2% after five desorption-regeneration cycles. The results of this process indicated that the removal percentage slowly diminished. Since CTAB-Z is a low price and easily found substance, attaining excellent adsorption performance is possible by properly increasing the amount of CTAB-Z.

3.7. Test with real hospital sewage

The study was performed using real wastewater. Real wastewater was collected from the entrance of a hospital treatment plant. The specifications of wastewater were pH of

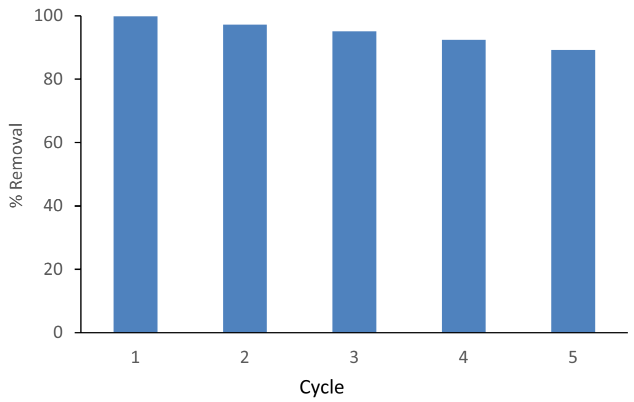

Fig. 10. Effect of regeneration on the adsorption of TC by CTAB-Z (time = 90 min, C_0 = 10 mg/L, pH = 7, dose = 1.5 g/L, temperature: 25°C).

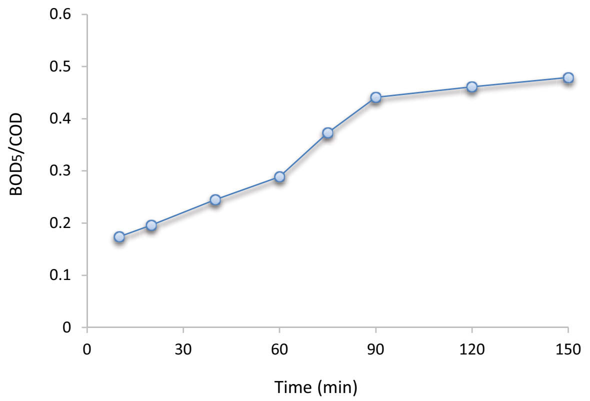

Fig. 11. Test with real sewage (Stirring rate = 200 rpm, dose = 1.5 g/L, temperature: 25°C).

5.5, COD of 620 mg/L, and BOD_5 of 108 mg/L; the BOD_5/COD ratio was 0.175, which indicative of non-biodegradability of the wastewater.

The test was performed under the optimal conditions obtained in the study, that is, stirring rate = 200 rpm, natural pH of 5.5 and CTAB-Z dosage of 1.5 g/L, and the results were shown in Fig. 11. As can be seen, the BOD_5/COD ratio has reached 0.48 at the end of process, and it can be said that, using the adsorption process, non-biodegradable wastewater adsorption process has become biodegradable, and it can be suggested that this process be used before biological processes in the treatment of conventional wastewater treatment plants.

4. Conclusion

Removal of TC using CTAB-Z in the adsorption process was evaluated in the present study. Batch system was considered for conducting adsorption studies, and the TC adsorption efficiency was investigated under variations of various experimental parameters. Using the FTIR analysis for characterizing the adsorbent, the possibility for the contribution of the functional group during the surface sorption process was detected. The highest removal efficiency of the studied pollutant was achieved at adsorbent dosages of 1.5 g/L, and the equilibrium time was 90 min. Among adsorption isotherms used for describing data of studied process, better fit for TC adsorption was observed to be related to Langmuir model. PSO model was identified as a better kinetic model for the studied process. According to thermodynamic studies, the negative and positive values were obtained for $\Delta G°$ and $\Delta H°$; these values are representative of the spontaneous and feasible nature and endothermic nature of sorption, respectively. Thus, developed CTAB-Z could be considered a low-cost, effective, and abundant adsorbent for removing TC.

Acknowledgements

The authors are grateful to the Zahedan University of Medical Sciences for the financial support of this study.

References

[1] D. Balarak, F.K. Mostafapour, Photocatalytic degradation of amoxicillin using UV/Synthesized NiO from pharmaceutical wastewater, Indones. J. Chem., 19 (2019) 211–218.
[2] T.J. Al-Musawi, A.H. Mahvi, A.D. Khatibi, Effective adsorption of ciprofloxacin antibiotic using powdered activated carbon magnetized by iron(III) oxide magnetic nanoparticles, J. Porous Mater., 28 (2021) 835–852.
[3] D. Balarak, H. Azarpira, F.K. Mostafapour, Adsorption kinetics and equilibrium of ciprofloxacin from aqueous solutions using *Corylus avellana* (Hazelnut) activated carbon, Int. J. Pharm. Technol., 8 (2016) 16664–16675.
[4] D. Avisar, O. Primor, I. Gozlan, H. Mamane, Sorption of sulfonamides and tetracyclines to montmorillonite clay, Water Air Soil Pollut., 209 (2010) 439–450.
[5] X. Zhu, D.C.W. Tsang, F. Chen, S. Li, X. Yang, Ciprofloxacin adsorption on graphene and granular activated carbon: kinetics, isotherms, and effects of solution chemistry, Environ Technol., 36 (2015) 3094–3102.
[6] A. Fakhri, S. Adami, Adsorption and thermodynamic study of Cephalosporins antibiotics from aqueous solution onto MgO nanoparticles, J. Taiwan Inst. Chem. Eng., 45 (2014) 1001–1006.
[7] D. Balarak, A.H. Mahvi, M.J. Shim, S.-M. Lee, Adsorption of ciprofloxacin from aqueous solution onto synthesized NiO: isotherm, kinetic and thermodynamic studies, Desal. Water Treat., 203 (2020) 1–11.
[8] H. Azarpira, Y. Mahdavi, O. Khaleghi, Thermodynamic studies on the removal of metronidazole antibiotic by multi-walled carbon nanotubes, Pharm. Lett., 8 (2016) 107–13.
[9] J.M. Cha, S. Yang, K.H. Carlson, Trace determination of β-lactam antibiotics in surface water and urban wastewater using liquid chromatography combined with electrospray tandem mass spectrometry, J. Chromatogr., A, 1115 (2006) 46–57.
[10] A.J. Watkinson, E.J. Murby, D.W. Kolpin, S.D. Costanzo. The occurrence of antibiotics in an urban watershed: From wastewater to drinking water, Sci. Total Environ., 407 (2009) 2711–2723.
[11] A.H. Mahvi, F.K. Mostafapour, Biosorption of tetracycline from aqueous solution by *Azolla filiculoides*: equlibrium kinetic and thermodynamic studies, Fresenius Environ. Bull., 27 (2018) 5759–5767.
[12] D. Balarak, H. Azarpira, F.K. Mostafapour, Adsorption isotherm studies of tetracycline antibiotics from aqueous solutions by maize stalks as a cheap biosorbent, Int. J. Pharm. Technol., 8 (2016) 16664–16675.
[13] Y. Gao, Y. Li, L. Zhang, H. Huang, J. Hu, S.M. Shah, X. Su, Adsorption and removal of tetracycline antibiotics from aqueous solution by graphene oxide, J. Colloid Interface Sci., 368 (2012) 540–546.
[14] M.E. Parolo, M.C. Savini, J.M. Vallés, M.T. Baschini, M.J. Avena, Tetracycline adsorption on montmorillonite: pH and ionic strength effects, Appl. Clay Sci., 40 (2008) 179–186.

[15] L.T. Popoola, Tetracycline and sulfamethoxazole adsorption onto nanomagnetic walnut shell-rice husk: isotherm, kinetic, mechanistic and thermodynamic studies, Int. J. Environ. Anal. Chem., 100 (2019) 1–23.
[16] A. Mariyam, J. Mittala, F. Sakina, R.T. Baker, A.K. Sharma, Adsorption behaviour of Chrysoidine R dye on a metal/halide-free variant of ordered mesoporous carbon, Desal. Water Treat., 223 (2021) 425–433.
[17] Anastopoulos, I. Pashalidis, A.G. Orfanos, I.D. Manariotis, A. Mittal, A.N. Delgadog, Removal of caffeine, nicotine and amoxicillin from (waste)waters by various adsorbents. A review, J. Environ. Manage., 261 (2020) 110236.
[18] J. Mittal. Recent progress in the synthesis of Layered Double Hydroxides and their application for the adsorptive removal of dyes: a review, J. Environ. Manage., 295 (2021) 113017.
[19] A. Mariyam, J. Mittal, F. Sakina, R.T. Baker, A.K. Sharma, A. Mittal, Efficient batch and Fixed-Bed sequestration of a basic dye using a novel variant of ordered mesoporous carbon as adsorbent, Arabian J. Chem., 14 (2021) 103186.
[20] A. Mittal, R. Ahmad, I. Hasan, Iron oxide-impregnated dextrin nanocomposite: synthesis and its application for the biosorption of Cr(VI) ions from aqueous solution, Desal. Water Treat., 57 (2015) 15133–15145.
[21] P. Saharan, V. Kumar, J. Mittal, V. Sharma, A.K. Sharma, Efficient ultrasonic assisted adsorption of organic pollutants employing bimetallic-carbon nanocomposites, 56 (2021) 1866608, doi: 10.1080/01496395.2020.1866608.
[22] D. Balarak, H. Azarpira. Photocatalytic degradation of sulfamethoxazole in water: investigation of the effect of operational parameters, Int. J. ChemTech. Res., 9 (2016) 566–573.
[23] S. Wang, E. Ariyanto, Competitive adsorption of malachite green and Pb ions on natural zeolite, J. Colloid Interface Sci., 314 (2007) 25–31.
[24] A. Martucci, I. Pasti, N. Marchetti, A. Cavazzini, F. Dondi, A. Alberti, Adsorption of pharmaceuticals from aqueous solutions on synthetic zeolites, Microporous Mesoporous Mater., 148 (2012) 174–183.
[25] I. Braschia, S. Blasioli, L. Gigli, C.E. Gessa, A. Alberti, A. Martucci, Removal of sulfonamide antibiotics from water: Evidence of adsorption into an organophilic zeolite Y by its structural modifications, J. Hazard. Mater., 178 (2010) 218–225.
[26] P.H. Chang, Z. Li, J.S. Jean, W.T. Jiang, C.J. Wang, K.H. Lin, Adsorption of tetracycline on 2:1 layered non-swelling clay mineral illite, Appl. Clay Sci., 67 (2012) 158–163.
[27] Y. Gao, Y. Li, L. Zhang, H. Huang, J. Hu, S.M. Shah, Adsorption and removal of tetracycline antibiotics from aqueous solution by graphene oxide, J. Colloid Interface Sci., 368 (2012) 540–546.
[28] K. Rahmani, M.A. Faramarzi, A.H. Mahvi, M. Gholam, A. Esrafili, H. Forootanfar, Elimination and detoxification of sulfathiazole and sulfamethoxazole assisted by laccase immobilized on porous silica beads, Int. Biodeterior. Biodegrad., 97 (2015) 107–114.
[29] M.E. Parolo, M.C. Savini, J.M. Vallés, M.T. Baschini, M.J. Avena, Tetracycline adsorption on montmorillonite: pH and ionic strength effects, Appl. Clay Sci., 40 (2008) 179–186.
[30] C. Arora, P. Kumar, S. Soni, J. Mittal, A. Mittal, B. Singh, Efficient removal of malachite green dye from aqueous solution using *Curcuma caesia* based activated carbon, Desal. Water Treat., 195 (2020) 341–352.
[31] S. Soni, P.K. Bajpai, D. Bharti, J. Mittal, C. Arora, Removal of crystal violet from aqueous solution using iron based metal organic framework, Desal. Water Treat., 205 (2020) 386–399.
[32] V.K. Gupta, S. Agarwal, R Ahmad, A. Mirza, J. Mittal, Sequestration of toxic congo red dye from aqueous solution using ecofriendly guar gum/activated carbon nanocomposite, Int. J. Biol. Macromol., 158 (2020) 1310–1318.
[33] X. Pan, C. Deng, D. Zhang, J. Wang, G. Mu, Y. Chen, Toxic effects of amoxicillin on the photosystem II of *Synechocystis* sp. characterized by a variety of in vivo chlorophyll fluorescence tests, Aquat. Toxicol., 89 (2008) 207–213.
[34] H. Tekin, O. Bilkay, S.S. Ataberk, T.H. Balta, I.H. Ceribasi, F.D. Sanin, U. Yetis, Use of Fenton oxidation to improve the biodegradability of a pharmaceutical wastewater, J. Hazard. Mater., 136 (2006) 258–265.
[35] X.S. Wang, Y. Zhou, Y. Jiang, C. Sun, The removal of basic dyes from aqueous solutions using agricultural by-products, J. Hazard. Mater., 157 (2008) 374–385.
[36] L.A. Al-Khateeb, S. Almotiry, M.A. Salam, Adsorption of pharmaceutical pollutants onto graphene nanoplatelets, Chem. Eng. J., 248 (2014) 191–199.
[37] W.T. Jiang, P.H. Chang, Y.S. Wang, Y. Tsai, J.S. Jean, Z. Li, K. Krukowski, Removal of ciprofloxacin from water by birnessite, J. Hazard. Mater., 250 (2013) 362–369.
[38] Y.H. Lin, S. Xu, J. Li. Fast and highly efficient tetracycline removal from environmental waters by graphene oxide functionalized magnetic particles, Chem. Eng. J., 225 (2013) 679–685.
[39] P.H. Chang, Z.H. Li, T.L. Yu, S. Munkhbayer, T.H. Kuo, Sorptive removal of tetracycline from water by palygorskite, J. Hazard. Mater., 165 (2009)148–155.
[40] M. Brigante, P.C. Schulz, Remotion of the antibiotic tetracycline by titania and titania-silica composed material, J. Hazard. Mater., 192 (2011) 1597–1608.
[41] Y.P. Zhao, J.J. Geng, X.R. Wang, X.Y. Gu, S.X. Gao, Tetracycline adsorption on kaolinite: pH, metal cations and humic acid effects, Ecotoxicology, 20 (2011) 1141–1147.
[42] X. Yang, G.R. Xu, H.R. Yu, Z. Zhang, Preparation of ferric-activated sludge-based adsorbent from biological sludge for tetracycline removal, Bioresour. Technol., 211 (2012) 566–573.
[43] P. Liu, W.J. Liu, H. Jiang, JJ. Chen, W.W. Li, H.Q. Yu, Modification of bio-char derived fromfast pyrolysis of biomass and its application in removal of tetracycline from aqueous solution, Bioresour. Technol., 121 (2012) 235–240.
[44] J. Rivera-Utrilla, C.V. Gomez-Pacheco, M. Sonchez-Polo, J.J. Lopez-Peoalver, Tetracycline removal from water by adsorption/bioadsorption on activated carbons and sludge-derived adsorbents, Environ. Manage., 131 (2013) 16–24.
[45] L.L. Ji, W. Chen, L. Duan, D.Q. Zhu. Mechanisms for strong adsorption of tetracycline to carbon nanotubes: a comparative study using activated carbon and graphite as adsorbents, Environ. Sci. Technol., 43 (2009) 2322–2327.
[46] D. Balarak, E. Bazrafshan, Y Mahdavi, S.M. Lee, Kinetic, isotherms and thermodynamic studies in the removal of 2-chlorophenol from aqueous solution using modified rice straw, Desal. Water Treat., 63 (2017) 203–211.
[47] D. Balarak, F. Mostafapour, E. Bazrafshan, T.A. Saleh, Studies on the adsorption of amoxicillin on multi-wall carbon nanotubes, Water Sci. Technol., 75 (2017) 1599–1606.
[48] Y. Tang, H. Guo, L. Xiao, S. Yu, N. Gao, Y. Wang, Synthesis of reduced graphene oxide/magnetite composites and investigation of their adsorption performance of fluoroquinolone antibiotics, Colloids Surf., A, 424 (2013) 74–80.
[49] H. Chen, Z. Zhang, M. Feng, W. Liu, W. Wang, Q. Yang, Y. Hu, Degradation of 2,4-dichlorophenoxyacetic acid in water by persulfate activated with FeS (mackinawite), Chem. Eng. J., 313 (2017) 498–507.
[50] B.N. Estevinho, I. Martins, N. Ratola, A. Alves, L. Santos, Removal of 2,4-dichlorophenol and pentachlorophenol from waters by sorption using coal fly ash from a Portuguese thermal power plant, J. Hazard. Mater., 143 (2007) 535–540.
[51] S. Ahmadi, A. Banach, F.K. Mostafapour, Study survey of cupric oxide nanoparticles in removal efficiency of ciprofloxacin antibiotic from aqueous solution: adsorption isotherm study, Desal. Water Treat., 89 (2017) 297–303.
[52] D. Balarak, H. Azarpira, Rice husk as a Biosorbent for antibiotic metronidazole removal: isotherm studies and model validation, Int. J. ChemTech Res., 9 (2016) 566–573.
[53] D. Balarak, H. Azarpira, F.K. Mostafapour, Study of the adsorption mechanisms of cephalexin on to *Azolla filiculoides*, Pharm. Chem., 8 (2016) 114–121.
[54] F.A. Adekola, H.I. Adegoke, G.B. Adebayo, I.O. Abdulsalam, Batch sorption of ciprofloxacin on kaolinitic clay and nhematite composite: equilibrium and thermodynamics studies, Mor. J. Chem., 4 (2016) 384–424.

[55] L. Wang, G. Chen, C. Ling, J. Zhang, K. Szerlag, Adsorption of ciprofloxacin on to bamboo charcoal: effects of pH, salinity, cations, and phosphate, Environ. Prog. Sustain., 36 (2017) 1108–1115.
[56] D. Balarak, Z. Taheri, M.J. Shim, S.M. Lee, C. Jeon, Adsorption kinetics and thermodynamics and equilibrium of ibuprofen from aqueous solutions by activated carbon prepared from *Lemna minor*, Desal. Water Treat., 215 (2021) 183–193.
[57] D. Balarak, M. Baniasadi, S.M. Lee, M.J. Shim, Ciprofloxacin adsorption onto *Azolla filiculoides* activated carbon from aqueous solutions, Desal. Water Treat., 218 (2021) 444–453.
[58] A.D. Khatibi, A.H. Mahvi, N. Mengelizadeh, Adsorption-desorption of tetracycline onto molecularly imprinted polymer: isotherm, kinetics, and thermodynamics studies, Desal. Water Treat., 230 (2021) 240–251.
[59] A. Meshkinain, B. Davoud, Y. Nastaran, Optimization of nickel oxide nanoparticle synthesis through the sol-gel method for adsorption of Penicillin G, Res. J. Chem. Environ., 25 (2021) 31–36.